

# Partonic structure of $\gamma_L^*$ in hard collisions

Jiří Chýla\*

\* *Research Center for Particle Physics, Institute of Physics of the Academy of Sciences  
18221 Na Slovance 2, Prague 8, Czech Republic*

**Abstract.** Manifestation of QCD improved partonic structure of longitudinally polarized virtual photons in hard collisions is discussed. As an example, dijet production in ep collisions at HERA is investigated in detail.

## INTRODUCTION

In this talk I discuss phenomenological consequences of QCD improved partonic structure of longitudinally polarized virtual photons ( $\gamma_L^*$ ), concentrating on LO QCD calculations of dijet production in ep collisions at HERA. Some of the results presented here are discussed in detail in [1–3]. The role of resolved  $\gamma_L^*$  in NLO QCD calculations will be addressed elsewhere [4]. I start by recalling the virtue of extending the concept of partonic “structure” to virtual photons [5,6]:

- In principle, the concept of partonic structure of virtual photons can be dispensed with as higher order QCD corrections to cross sections of processes involving virtual photons in the initial state are well-defined and finite even for massless partons.
- In practice, however, the concept of *resolved virtual photon* is extraordinarily useful as it allows us to include the resummation of higher order QCD effects that come from physically well-understood region of (almost) parallel emission of partons off the quarks and antiquarks coming from the primary  $\gamma^* \rightarrow q\bar{q}$  splitting and subsequently participating in hard processes.

For the virtual photon, as opposed to the real one, its parton distribution functions (PDF) can therefore be regarded as “merely” describing higher order perturbative effects and not their “genuine” structure. Although this distinction between the content of PDF of real and virtual photons exists, it does not affect the *phenomenological* usefulness of PDF of the virtual photon. As shown in [5] the nontrivial part of the contributions of resolved  $\gamma_T^*$  to NLO calculations of dijet production at HERA is large and affects significantly the conclusions of phenomenological analyses of existing experimental data. Taking into account resolved  $\gamma_L^*$  turns out to be phenomenologically important as well.

## PARTON DISTRIBUTION FUNCTIONS OF $\gamma_L^*$ IN QCD

Most of the present knowledge of the structure of the photon comes from experiments at ep and  $e^+e^-$  colliders, where the incoming leptons act as sources of transverse ( $\gamma_T^*$ ) and longitudinal ( $\gamma_L^*$ ) virtual photons of virtuality  $P^2$  and momentum fraction  $y$ . To order  $\alpha$  their respective unintegrated fluxes are given as

$$f^{\gamma_T^*}(y, P^2) = \frac{\alpha}{2\pi} \left( \frac{1 + (1 - y)^2}{y} \frac{1}{P^2} - \frac{2m_e^2 y}{P^4} \right), \quad (1)$$

$$f^{\gamma_L^*}(y, P^2) = \frac{\alpha}{2\pi} \frac{2(1 - y)}{y} \frac{1}{P^2}. \quad (2)$$

Phenomenological analyses of interactions of virtual photons and their PDF have so far concentrated on  $\gamma_T^*$ . Neglecting longitudinal photons is a good approximation for  $y \rightarrow 1$ , where  $f^{\gamma_L^*}(y, P^2) \rightarrow 0$ , as well as for small virtualities  $P^2$ , where PDF of  $\gamma_L^*$  vanish by gauge invariance. But how small is “small” in fact? For instance, should we take into account the contribution of  $\gamma_L^*$  to jet cross sections in the region  $E_T \gtrsim 5$  GeV,  $P^2 \gtrsim 1$  GeV<sup>2</sup>, where most of the data on virtual photons obtained in ep collisions at HERA come from? The present paper is devoted primarily to addressing this question.

In pure QED and to order  $\alpha$  the probability of finding inside  $\gamma_L^*$  of virtuality  $P^2$  a quark with mass  $m_q$ , charge  $e_q$ , momentum fraction  $x$  and virtuality  $\tau \leq M^2$ , is given, in units of  $3e_q^2\alpha/2\pi$ , as [5]

$$q_L^{\text{QED}}(x, m_q^2, P^2, M^2) = \frac{4x^2(1 - x)P^2}{\tau^{\min}} \left( 1 - \frac{\tau^{\min}}{M^2} \right), \quad (3)$$

where  $\tau^{\min} = xP^2 + m_q^2/(1 - x)$ . The quantity defined in (3) has a clear physical interpretation: it describes the flux of quarks that are almost collinear with the incoming photon and “live” longer than  $1/M$ . For  $\tau^{\min} \ll M^2$  (3) simplifies to

$$q_L^{\text{QED}}(x, m_q^2, P^2, M^2) = \frac{4x^2(1 - x)P^2}{xP^2 + m_q^2/(1 - x)},$$

which for  $x(1 - x)P^2 \gg m_q^2$  further reduces to

$$q_L^{\text{QED}}(x, 0, P^2, M^2) = 4x(1 - x), \quad (4)$$

whereas for  $x(1 - x)P^2 \ll m_q^2$

$$q_L^{\text{QED}}(x, m_q^2, P^2, M^2) \rightarrow \frac{P^2}{m_q^2} 4x^2(1 - x)^2.$$

QCD corrections to QED expressions for PDF of  $\gamma_L^*$  have been derived in leading-logarithmic approximation in the region  $1 \lesssim P^2 \ll M^2$  in [2]. By “leading-log” I

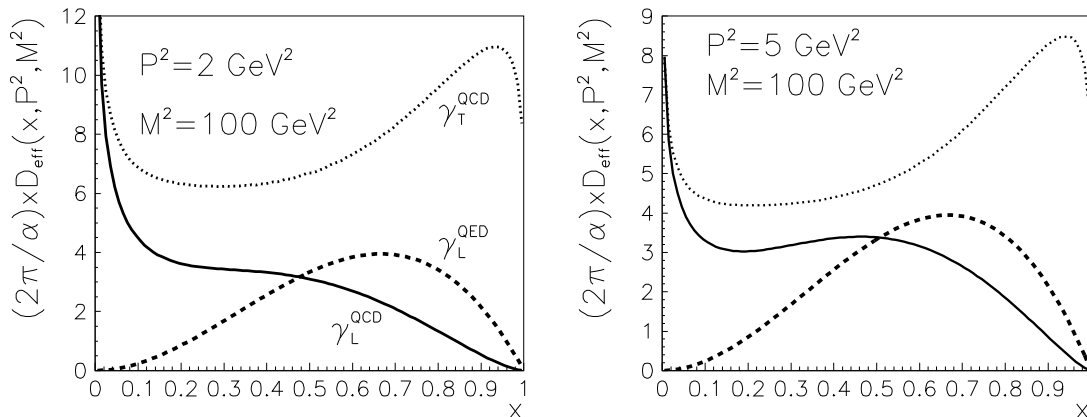


**FIGURE 1.** Comparison of the contributions of resolved  $\gamma_T^*$  and  $\gamma_L^*$  to  $D_{\text{eff}}$  defined in (5) for  $M^2 = 100 \text{ GeV}^2$  and  $P^2 = 2, 5 \text{ GeV}^2$ . QED and QCD formulae discussed in the text were used for  $\gamma_L^*$  and SaS1D parameterization for  $\gamma_T^*$ .

mean resummation of the terms  $(\alpha_s \ln M^2)^k$  at each order  $k$  of perturbative QCD. Note that for  $\gamma_T^*$  there is one power of  $\ln M^2$  more at each order of  $\alpha_s$ , the additional one coming from the primary QED  $\gamma^* \rightarrow q\bar{q}$  splitting. In the case of  $\gamma_L^*$  the analogous splitting gives rise to “constant” term (4), hence the absence of this log. The resulting expressions exhibit typical hadronic form of scale dependence and contain  $\Lambda_{\text{QCD}}$  as the only free parameter. QCD effects thus suppress quark distribution functions  $q_L^{\text{QED}}(x, P^2, M^2)$  at large  $x$  and enhance it on the other hand for  $x \lesssim 0.4$ . Moreover, they generate sizable gluon distribution function, absent in QED. The presence of the term proportional to  $\ln M^2$  in the expressions for  $q_T$  in both QED and QCD implies the dominance of  $\gamma_T^*$  at large  $M^2$ , but one would have to go to very large  $M^2$  for  $\gamma_L^*$  to become really negligible with respect to  $\gamma_T^*$ . For fixed  $M^2$  the relative importance of  $\gamma_L^*$  with respect to  $\gamma_T^*$  grows with  $P^2$ , but to retain clear physical meaning of PDF we stay throughout this paper in the region where  $P^2 \ll M^2$ . The lower bound  $1 \text{ GeV}^2 \lesssim P^2$  ensures that hadronic parts of QCD improved PDF of  $\gamma_L^*$ , which have not been taken into account in [2], can be safely neglected.

## $\gamma_L^*$ IN HARD COLLISIONS

The relevance of resolved  $\gamma_L^*$  in hard collisions of virtual photons depends on the theoretical framework we are working in. In this talk I will stay within the framework of LO QCD calculations of dijet production at HERA. The measurement of dijet cross sections in ep (and  $e^+e^-$ ) collisions offers currently the best way of investigating interactions of virtual photons [7,8]. In general the corresponding cross

sections are given as sums of contributions of all possible parton level subprocess. The simplest way of demonstrating the importance of the contributions of resolved  $\gamma_L^*$  employs the approximation [9] in which dijet cross sections are expressed in terms of single *effective parton distribution function* of the photon ( $\gamma_T^*$  or  $\gamma_L^*$ )

$$D_{\text{eff}}(x, P^2, M^2) \equiv \sum_{i=1}^{n_f} \left( q_i(x, P^2, M^2) + \bar{q}_i(x, P^2, M^2) \right) + \frac{9}{4} G(x, P^2, M^2), \quad (5)$$

where the factorization scale  $M$  is conventionally identified with (a multiple of) jet  $E_T$ :  $M = \kappa E_T$ . In Fig. 1 the contributions to  $D_{\text{eff}}$  of  $\gamma_L^*$ , evaluated with both QED and QCD formulae for its PDF, are compared to those of  $\gamma_T^*$  using SaS1D parameterization [10]. The comparison is performed for two pairs of  $P^2$  and  $M^2$  typical for HERA experiments. In addition to softening effects at large  $x$ , QCD improved PDF of  $\gamma_L^*$  give sizable contribution to  $D_{\text{eff}}$  at small  $x$  that comes from the gluon content of  $\gamma_L^*$ . Fig. 1 moreover suggests that in the region accessible at HERA the contributions of resolved  $\gamma_L^*$  are numerically important, particularly after incorporating QCD effects in its PDF.

After this simple but approximate estimate of the contributions of resolved  $\gamma_L^*$ , I now turn to the evaluation of dijet cross sections at HERA using complete LO QCD formalism as implemented in HERWIG 5.9 event generator. To include the effects of resolved  $\gamma_L^*$  I have added the option of generating the flux of  $\gamma_L^*$  combined with the call to QED or QCD improved PDF of  $\gamma_L^*$ . For  $\gamma_T^*$  the SaS1D PDF [10] were used. The dijet cross sections were evaluated for  $0.05 \leq y \leq 0.95$  in three windows of  $P^2$

$$1.4 \leq P^2 \leq 2.4 \text{ GeV}^2, \quad 2.4 \leq P^2 \leq 4.4 \text{ GeV}^2, \quad 4.4 \leq P^2 \leq 10 \text{ GeV}^2$$

and imposing the following cuts on jet  $E_T$  (all quantities are in  $\gamma^*p$  cms)

$$E_T^{(1)}, E_T^{(2)} \geq E_T^c, \quad E_T^c = 5, 10 \text{ GeV}.$$

The effects of H1 and ZEUS detector acceptances were taken into account by performing all calculations without any restrictions on  $\eta$  as well for  $-3 \leq \eta \leq 0$ .

The results presented in Figs. 2 and 3 correspond to parton level calculations in the first window of  $P^2$ , without and with the mentioned cuts on  $\eta$ . The characteristic dependence of the contributions of resolved  $\gamma_L^*$  on  $y$  is illustrated by plotting for each of the distributions in  $\eta$ ,  $E_T$  and  $x_\gamma$  also its ratio to that of  $\gamma_T^*$  for the whole interval  $0.05 \leq y \leq 0.95$ , as well as for three indicated subintervals. Except for  $x_\gamma$  close to 1, QCD improved PDF of  $\gamma_L^*$  enhance its contributions to dijet cross sections compared to those based on the purely QED. For  $y \lesssim 0.5$  they amount to about 50% of those of  $\gamma_T^*$ . For  $x_\gamma \lesssim 0.2$  this number increases further up to about 70%. Reducing the range of  $\eta$  to  $-3 \leq \eta \leq 0$  affects mainly the distribution  $d\sigma/dx_\gamma$  by suppressing it at both edges of the phase space. The ratios of the contributions of  $\gamma_L^*$  and  $\gamma_T^*$  are, however, affected only little by this cut.

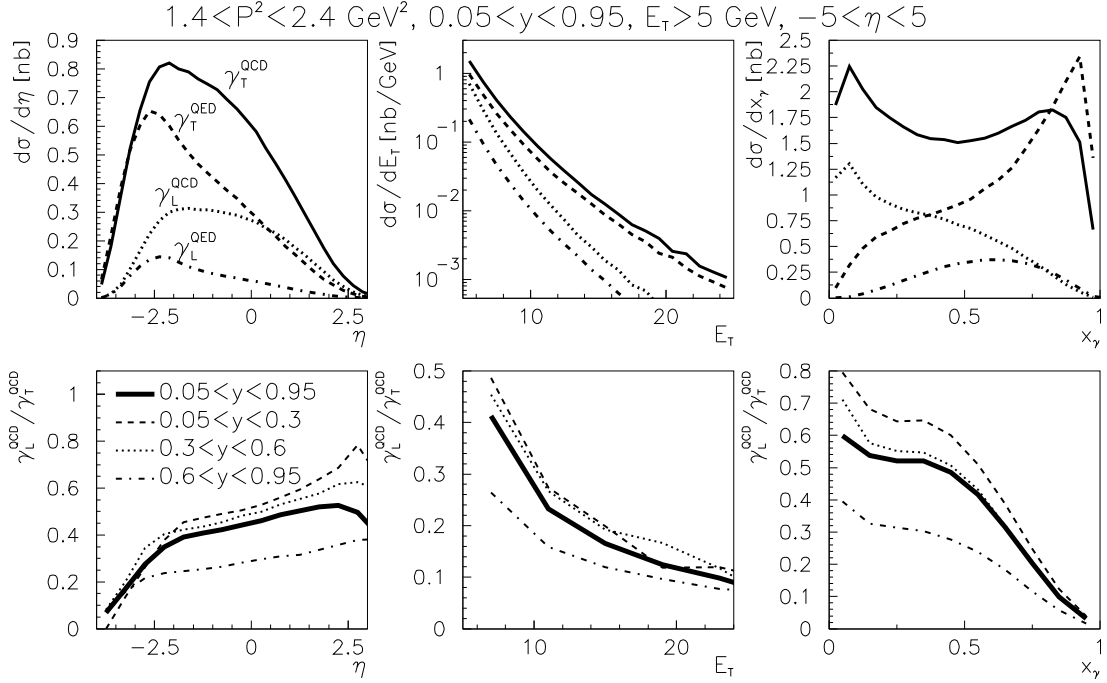


**FIGURE 2.** Upper three plots: dijet cross sections, corresponding to resolved  $\gamma_T^*$  and  $\gamma_L^*$  plotted as functions of  $\eta$ ,  $E_T$  and  $x_\gamma$  for  $1.4 \leq P^2 \leq 2.4 \text{ GeV}^2$ ,  $0.05 \leq y \leq 0.95$ ,  $E_T \geq 5 \text{ GeV}$ , without any restriction on  $\eta$ . Lower three plots: the corresponding ratio of the contributions of  $\gamma_L^*$  and  $\gamma_T^*$ , integrated over the whole interval  $0.05 \leq y \leq 0.95$ , as well as in three indicated subintervals.

Increasing the photon virtuality  $P^2$  enhances, approximately uniformly in the whole phase space, the relative importance of  $\gamma_L^*$  with respect to  $\gamma_T^*$ . On the contrary, rising the threshold  $E_T^c$  from 5 GeV to 10 GeV reduces it by a factor of about 2, since large  $E_T$  require large  $x_\gamma$ , where quarks from  $\gamma_T^*$  dominate.

The effects of hadronization on parton level results discussed above have been studied in detail in [8]. They are reasonably small ( $\lesssim 10 - 20\%$ ) and model independent in the region  $-2.5 \lesssim \eta$  but turn large and model dependent below that value. For the comparison with theoretical calculations the lower limit on accessible range of  $\eta$  enforced by H1 and ZEUS acceptances presents therefore no real restriction. On the other hand, it would be very useful to push the upper limit on  $\eta$  above  $\eta \simeq 0$  since the relevance of  $\gamma_L^*$  grows with  $\eta$ .

Summarizing the message of this Section, we conclude that for  $\Lambda^2 \ll P^2 \ll E_T^2$ :

- The contributions of  $\gamma_L^*$  are substantial, particularly for small  $y$ , large  $P^2$ , low  $E_T$  and small  $x_\gamma$ .
- The cuts enforced by H1 and ZEUS acceptances reduce the sensitivity to  $\gamma_L^*$ , but its contributions still make up typically 50% of those of  $\gamma_T^*$  and can be identified by their characteristic  $y$  and  $P^2$  dependencies.

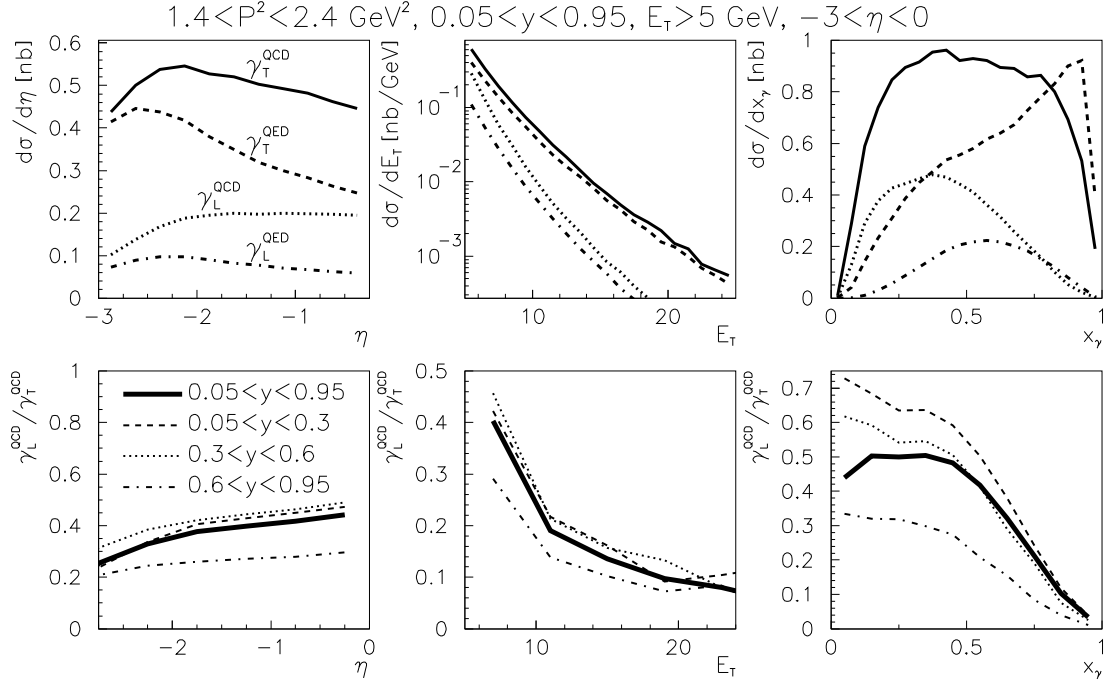


**FIGURE 3.** The same as in Fig. 2, but the restricted region  $-3 \leq \eta \leq 0$ .

## CONCLUSIONS

The contributions of resolved  $\gamma_L^*$  to dijet production in ep collisions at HERA were evaluated using QCD improved PDF of  $\gamma_L^*$  constructed recently. In the region accessible at HERA they turn out to sizable, amounting typically to 50% of those from  $\gamma_T^*$ , and depend sensitively of  $y$ ,  $E_T$  and  $x_\gamma$ .

Work performed under the project LN00A006 of the Ministry of Education of the Czech Republic

## REFERENCES

1. Chýla, J., and Taševský, M., *Eur. Phys. J.* **C16**, 471 (2000).
2. Chýla, J., *Phys. Lett.* **B488**, 289 (2000).
3. Friberg, C., and Sjöstrand, T., LU TP 00-31, hep-ph/0009003.
4. Chýla, J., and Taševský, M., in preparation.
5. Chýla, J., and Taševský, M., *Phys. Rev.* **D**, (2000) in print, hep-ph/9912245.
6. Friberg, C., and Sjöstrand, T., *Eur. Phys. J.* **C13**, 151 (2000).
7. Adloff, C., et al. (H1 Collab.), *Eur. Phys. J.* **C13**, 397 (2000).
8. Taševský, M., PhD Thesis, Charles University, Prague, 1999.
9. Combridge, B.V., and Maxwell, C.J., *Nucl. Phys.* **B239**, 429 (1984).
10. Schuler, G., and Sjöstrand, T., *Z. Phys.* **C68**, 607 (1995).